Published in final edited form as:
Neuropharmacology. 2010 ; 59(1-2): 58–69. doi:10.1016/j.neuropharm.2010.03.016.

Mechanisms of inhibition of $Ca_V3.1$ T-type calcium current by aliphatic alcohols

Veit-Simon Eckle[a,d] and **Slobodan M Todorovic**[a,b,c,*]

[a]Department of Anesthesiology, University of Virginia Health System, School of Medicine, Charlottesville, VA

[b]Department of Neuroscience, University of Virginia Health System, School of Medicine, Charlottesville, VA

[c]Department of Neuroscience Graduate Program, University of Virginia Health System, School of Medicine, Charlottesville, VA

[d]Department of Anesthesiology, Klinikum rechts der Isar, Technische Universität München, Munich, Germany

Abstract

Many aliphatic alcohols modulate activity of various ion channels involved in sensory processing and also exhibit anesthetic capacity *in vivo*. Although the interaction of one such compound, 1-octanol (octanol) with different T-type calcium channels (T-channels) has been described, the mechanisms of current modulation and its functional significance are not well studied. Using patch-clamp technique, we investigated the mechanisms of inhibition of T-currents by a series of aliphatic alcohols in recombinant human $Ca_V3.1$ (α1G) T-channel isoform expressed in human embryonic kidney (HEK) 293 cells and thalamocortical (TC) relay neurons in brain slices of young rats. Octanol, 1-heptanol (heptanol) and 1-hexanol (hexanol) inhibited the recombinant $Ca_V3.1$ currents in concentration-dependent manner yielding IC_{50} values of 362 μM, 1063 μM and 3167 μM, respectively. Octanol similarly inhibited native thalamic $Ca_V3.1$ T-currents with an IC_{50} of 287 μM and diminished burst firing without significant effect on passive membrane properties of these neurons. Inhibitory effect of octanol on T-currents in both native and recombinant cells was accompanied with accelerated macroscopic inactivation kinetics and hyperpolarizing shift in the steady-state inactivation curve. Additionally, octanol induced a depolarizing shift in steady-state activation curves of T-current in TC neurons. Surprisingly, the recovery from fast inactivation at hyperpolarized membrane potentials was accelerated by octanol up three-fold in native but not recombinant channels. Given the importance of thalamocortical pathways in providing sleep, arousal, and anesthetic states, modulation of thalamic T-currents may at least contribute to the pharmacological effects of aliphatic alcohols.

[*]**Correspondence:** Slobodan M. Todorovic, Department of Anesthesiology, University of Virginia Health System, Mail Box 800710, Charlottesville, VA 22908-0710, Phone: 434-924-2283, Fax: 434-982-0019, st9d@virginia.edu.

DISCLOSURES

The authors confirm that the presented study was performed without any conflict of interest.

INTRODUCTION

Recent work indicates that studies of ion channels expressed in the thalamus, as well as the neuronal circuits that regulate its activity, can advance our knowledge of how anesthetics cause loss of consciousness. Voltage-gated Ca^{2+} channels have the important function of controlling cellular excitability and transmitter release in CNS neurons. T-currents have a significant role in generating thalamic low-threshold calcium spikes (LTCS), which evoke burst firing of sodium-dependent fast spikes (Sherman, 2005; Steriade , 2005; Perez-Reyes, 2003). Some classes of general anesthetics depress currents arising from these channels at clinically relevant concentrations (Todorovic and Lingle, 1998; Todorovic et al., 2000; Takenoshita and Steinbach, 1991; Herrington and Lingle, 1992). However, the mechanisms of particular Ca^{2+} current inhibition by diverse classes of anesthetics have not been well studied. Furthermore, T-type calcium channels (T-channels) that activate with small membrane depolarization are abundantly expressed in thalamic neurons and have a central function in the generation of rhythmic thalamocortical oscillations. In turn, these oscillations control consciousness and cognition (Angel, 1991; McCormick and Bal, 1997; Steriade, 2005; Alkire et al., 2000), as well as abnormal excitability that can contribute to seizures, neurogenic pain, and other neuropsychiatric disorders termed “thalamocortical dysrhythmias” (Llinas et al., 1998). Hence, better definition of the pharmacological properties of T-currents in thalamic neurons and the biophysical mechanisms of their modulation could be of major importance in defining the physiological functions of these currents and their participation in the effects of clinical drugs such as anesthetics, anticonvulsants, and analgesics.

Thalamocortical relay (TC) neurons exhibit two functional firing modes: tonic firing, which is thought to predominate during wakefulness, and burst firing, which is thought to be mostly associated with sleep states (McCormick and Bal, 1997). However, evidence strongly suggests that both firing modes of TC neurons can be present during awake states (reviewed by Sherman, 2005). Switching of these firing patterns might be crucially involved in different states of sleep, wakefulness and anesthesia (Franks, 2008).

Many common alcohols have an anesthetic capacity in different animals and are used to probe for molecular targets of anesthesia. 1-Octanol (octanol), a straight- chain fatty alcohol with eight carbon atoms and other related alcohols, displays anesthetic properties *in vivo* (Alifimoff et al., 1989). It has been suggested that octanol may affect several classes of ion channels thought to be relevant targets for anesthetics. For example, octanol potentiates $GABA_A$-receptor-gated currents, one of the major cellular targets of general anesthesia (Franks and Lieb, 1994). However, octanol also inhibits T-currents in adult dorsal root ganglion cells (Todorovic and Lingle, 1998), GH_3 cell lines (Herrington and Lingle, 1992), hippocampal neurons (Takahashi et al., 1989), TC neurons (Llinas et al., 2007) and reticular thalamic neurons (Joksovic et al., 2010). Furthermore, TC neurons of the ventral posterior thalamic nucleus express a large T-current that is most likely mediated by the highly expressed α1G ($Ca_V3.1$) calcium channel subunit (Talley et al., 1999; Kim et al., 2001). We previously found that recombinant rat $Ca_V3.1$ currents are also inhibited by octanol at clinically relevant concentrations (Todorovic et al., 2000). However, in previous studies, mechanisms of the interaction of octanol with $Ca_V3.1$ T-currents have not been extensively studied. Given the proposed importance of the thalamus in sensory processing and anesthetic states, we examined the biophysical mechanism underlying the effect of octanol on recombinant human $Ca_V3.1$ and native T-current in the TC neurons of ventrobasal thalamic nucleus, the main sensory structure in the thalamus.

MATERIALS AND METHODS

In vitro tissue slice preparation

Experiments were done in accordance with institutional and federal guidelines, including the National Institutes of Health guide for the care and use of Laboratory animals (NIH Publications No. 8023, revised 1978). Our *in vitro* slice preparation technique has been described previously (Joksovic et al., 2005). Briefly, young Sprague-Dawley rats of either sex (postnatal days 8–15) were anesthetized with isoflurane, then decapitated. Brain tissue was rapidly removed and placed in ice-cold slicing solution containing (in mM) 260 sucrose, 26 $NaHCO_3$, 10 D-glucose, 3 KCl, 1.25 NaH_2PO_4, 2 $MgCl_2$, and 2 $CaCl_2$, adjusted to pH 7.4 with carbogen gas (95% O_2-5% CO_2). Coronal slices (300 μm thick) containing the sensory ventral posteromedial and posterolateral thalamic nuclei (stereotaxic levels −2.85 to −3.70 mm below bregma) (Swanson, 1992) were cut on a microslicer (NVSLM1, World Precision Instruments, Sarasota, FL) and incubated for 30 min in 35°C artificial cerebrospinal fluid containi ng (in mM) 124 NaCl, 4 KCl, 26 $NaHCO_3$, 1.25 NaH_2PO_4, 2 $MgCl_2$, 10 D-glucose, and 2 $CaCl_2$ adjusted to pH 7.4 with carbogen gas. After incubation, slices were held at room temperature at least 45 min before recording procedures.

Recording procedures

HEK-293 cells—For recordings of recombinant T-currents, we used stably-expressed human $Ca_V3.1a$ isoform of channels, which is widely expressed in the brain including the thalamus (Monteil et al., 2000). The clones are expressed in human embryonic kidney 293 (HEK-293) cells as reported previously (Joksovic et al., 2006; Orestes et al., 2009). HEK-293 cells (CRL-1573; American Type Culture Collection, Manassas, VA) were grown in DMEM/F-12 media (Invitrogen) supplemented with 10% fetal bovine serum, penicillin G (100mg/ml), and streptomycin (0.1mg/ml).

Brain slices—Slices were placed in a recording chamber (1-ml bath volume, RC-24N, Warner Instruments, Hamden, CT) that was steadily superfused at a rate of 2 ml/min with carbogenated recording solution containing (in mM) 125 NaCl, 1 $MgCl_2$, 25 D-glucose, 25 $NaHCO_3$, 1.25 NaH_2PO_4, 2.5 KCl, 2 $CaCl_2$, and 0.001 tetrodotoxin. Saturation with carbogen gas led to a pH of 7.4. For experiments with isoflurane, this external solution was bubbled continuously during recording with bubbling stone attached with tygon tubing to the agent-specific vaporizer with a constant flow of carbogen gas. All recordings were done at room temperature. Thalamocortical relay neurons of the ventral posterior thalamic nucleus were visually identified by videomicroscopy (high- performance CCD camera, Cohu, San Diego, CA) combined with a BX51WI microscope with oblique illumination (Olympus, Hamburg, Germany). Intracellular solution for voltage-clamp recordings contained in mM, 90 tetramethylammonium-OH, 10 EGTA, 40 HEPES, 2 $MgCl_2$, 45 Cs-methane-sulfonate, 5 Mg-ATP, and 0.3 Tris-GTP titrated to pH 7.15–7.25 with hydrofluoric (HF) acid (Joksovic et al. 2005). Same internal and external solutions were used for voltage-clamp recordings of recombinant $Ca_V3.1$ currents. For current-clamp recording in brain slices we used the same external solution (except that tetrodotoxin was not included) and internal solution contained (in mM): 130 potassium gluconate, 5 EGTA, 4 NaCl, 10 HEPES, 0.5 $CaCl_2$, 2 Mg-ATP, 0.3 Tris-GTP. Measured liquid junction potentials in voltage-clamp experiments were −1.30 ± 0.10 mV (n=4) and in current-clamp experiments were −0.10 ± 0.05 mV (n=4).

Electrophysiological recordings

T-currents were obtained from TC neurons of the ventral posterior thalamic nucleus using whole-cell voltage clamp technique. We included recordings from 77 different cells. Each experiment was performed in a separate slice to prevent contamination with residual octanol. Thin-walled glass capillary electrodes (Corning 7056, Warner Instruments, Hamden, CT) had

initial resistances of 3–5 MΩ. For quality reasons, whole-cell configurations had to display gigaseal formation (≥2 GΩ). Series resistance and cell capacitance were compensated to the maximal possible extent. After equilibration with intracellular solution, currents were monitored by periodic voltage steps until the current stabilized. Recordings typically began 10 min after rupturing the membrane patch. We recorded membrane currents with a Multiclamp 700B patch-clamp amplifier (Molecular Devices, Foster City, CA) equipped with a CV-7B headstage. Voltage commands and the digitalization of membrane currents were done with Clampex 10.0 of the pClamp software package (Molecular Devices, Foster City, CA). Neurons were typically depolarized from holding potential (V_h) to test potential (V_t) of −50 mV every 20 s to evoke inward calcium currents. Records were filtered at 1.4 kHz with a low-pass filter (Bessel 8-pole).

Analysis of current

Results are presented as mean ± SEM (unless otherwise stated). The amplitude of T-current was measured from the peak, which was subtracted from the current at the end of the depolarizing test potential to avoid small contamination with residual high-voltage-activated (HVA) currents, which were resistant to intracellular hydrofluoric acid. Curve fitting was done with Origin 7.0 software (OriginLab, Northampton, MA). Concentration-response curves were fitted by the following Hill equation: $y = V_{max} [x^n / (IC_{50} + x^n)]$, where V_{max} is the maximal current block, IC_{50} the concentration that produces 50% of maximal inhibition, and n the apparent Hill coefficient for blockade. The voltage dependence of steady-state activation was described with a single Boltzmann distribution:

$$G(V)=G_{max}/(1+\exp[-(V - V_{50})/k])$$

where G_{max} is the maximal estimated conductance, V_{50} is the half-maximal voltage, and *k* (units of mV) represents the voltage dependence of the distribution. The voltage-dependence of steady-state inactivation was described with a single Boltzmann distribution:

$$I(V)=I_{max}/(1+\exp[(V - V_{50})/k])$$

where I_{max} is the maximal current, V_{50} is the half-maximal voltage, and *k* (units of mV) represents the voltage dependence of the distribution.

The time course of recovery from inactivation was fitted using a single-exponential equation: $y = A_1 * e^{(-x / t1)} + y_0$, where A_1 is the amplitude and t_1 the decay constant and y_0 the offset. Statistical analysis was performed with paired Student's *t*-test. Significant differences were determined by a level of $p < 0.05$.

Drugs and chemicals

Octanol, hexanol and heptanol were obtained from Sigma Chemical (St. Louis, MO). Stock solutions of 2 mM of alcohols were made in recording solution by stirring at least 12 h in a tightly sealed glass bottle. For experiments, appropriate external solution with each alcohol was freshly made from the stock solution after briefly vortexing. Tubing was made of tygon (S-54-HL, Norton Performance Plastics, Akron, OH) to minimize loss of drugs. For confirming appropriate concentrations of anesthetic alcohols in our *in vitro* experiments, recording solution containing nominal 2 mM octanol was measured after passing tygon tubing and collecting from the recording chamber. Gas chromatography-mass spectroscopy analysis (FAI Materials Testing Laboratory, Marietta, GA) showed about 10% lower concentration in two samples (1.75 mM, 1.84 mM). However, anesthetic delivery *in vitro* could be further compromised in tissue due to delicate diffusion into slices (Chesney et al., 2003). Thus, although our method

allows investigation of the effects of octanol in intact native cells, all quantitative assessments should be taken with caution. Actual effective concentrations of all drugs are likely to be much lower than those reported. Tetrodotoxin was obtained from Tocris Bioscience (Ellisville, MO). All other salts and chemicals were obtained either from Sigma Chemical (St. Louis, MO) or Fisher Scientific (Fair Lawn, NJ).

Solution exchange procedures

Multiple independently controlled glass syringes attached to the common tygon tubing served as reservoirs for a gravity-driven perfusion system. For experiments, flow was continuously maintained at 2 ml/min. Manually operated valves were used to switch solutions. Switching between perfusion syringes did not alter the amplitude or kinetics of T-current.

Methodological considerations relevant to intact brain slices

Recordings from intact brain slices offer great advantages for studying neurons in an intact setting *in vitro*. However, since voltage control is compromised in whole-cell recordings from slices due to the presence of extensive cell processes, we paid close attention to the signs of good voltage control. Specifically, there was no extensive delay in the onset of current; also, the onset and offset kinetics depended on voltage, not on the amplitude of current. In whole-cell experiments, because intact TC neurons have long processes, rapid components of recorded current, such as tail currents, are not likely to reflect the true amplitude and time course of Ca^{2+} current behavior. All our measurements of amplitudes from holding, peak, and steady-state currents were made at time points sufficient to ensure reasonably well-clamped current conditions. Furthermore, using brain slices from young animals, in which dendrites are not fully developed, alleviated the space-clamp problem.

RESULTS

Mechanisms of inhibition of recombinant human $Ca_V3.1$ currents by aliphatic alcohols

We first examined the ability of 3 aliphatic alcohols to inhibit recombinant human $Ca_V3.1$ currents in HEK293 cells. Figure 1A depicts representative traces (V_h −90 mV, V_t −30 mV) and Fig. 1B shows time course of the effect of 1 mM octanol which almost completely inhibited peak T-currents in HEK293 cells. At the same concentration heptanol (Fig. 1C and 1D) inhibited about 50% of recombinant $Ca_V3.1$ currents, and traces of Fig. 1E illustrate that 1 mM hexanol inhibited less than 10% of $Ca_V3.1$ currents. Figure 1F shows average concentration response curves for 3 aliphatic alcohols from multiple experiments with octanol (IC_{50} 362±44 μM) being about 3-fold more potent than heptanol (IC_{50} 1063±83 μM) and about 10-fold more potent than hexanol (IC_{50} 3167±329 μM). Note that slopes of the curves are similar and are depicted by parallel shift in the potency with longest alcohol molecule (octanol) being most potent in inhibiting recombinant T-currents.

Since octanol was most potent aliphatic alcohol in inhibiting recombinant $Ca_V3.1$ currents, we focused in further studies in native and recombinant cells on this compound. We did biophysical studies to discern the mechanisms of modulation of recombinant human $Ca_V3.1$ T-currents by octanol. Figure 2A shows traces of a family of inward currents evoked by progressive depolarizing steps from −80 to 30 mV from a holding potential (V_h) of −90 mV in control conditions and Fig. 2B shows traces during the application of 1 mM octanol in the same cell. Figure 2C depicts the average current-voltage (I-V) curves from 7 cells in experiments similar to those shown in Figs. 2A–B. It is evident that octanol depressed peak current over the range of all examined test potentials (V_t). From these experiments, we calculated the apparent voltage dependence of activation (Fig. 2D). The effect of octanol on the midpoint of activation (V_{50}) in these cells was only mildly shifted in depolarized potentials by about 3 mV (control −44.3 ±1.7 mV, octanol −41.3 ± 1.2 mV; n=7, $p>0.05$). From the I–V curves depicted above (Fig.

2C), we also examined macroscopic current kinetics of activation (Fig. 2E) and inactivation (Fig. 2F). We found that octanol significantly ($p<0.05$ by paired t-test) accelerated $Ca_V3.1$ channel activation kinetics at V_t −50 mV, −40 mV and −30 mV), as well as inactivation kinetics in all tested potentials from V_t −50 through 10 mV.

Concentration-dependent effect of octanol on T-currents in TC neurons

Traces depicted on Fig. 3A indicate that 1 mM octanol reversibly inhibited about 80% of T-current (V_h −100 mV, V_t −50 mV) in TC neurons of the ventral posterior thalamic nucleus. Similar to the effects on recombinant $Ca_V3.1$ current, inhibitory effect was accompanied with prominent speeding of macroscopic current inactivation kinetics. For example, at V_h −100 mV and V_t −50 mV, control τ was 25.0 ± 2.3 msec, and octanol τ was 14.3 ± 2.1 msec, (n=7, $p < 0.01$). In contrast, averaged 10–90 rise time in the same cells was not statistically significant: control = 4.5 ± 0.5 msec, octanol = 4.1 ± 0.6 msec ($p >0.05$). The average time course of 1 mM octanol application from 5 TC cells is depicted in Fig. 3*B*. Note that the time course of maximal inhibition of T-current with octanol was slower than in HEK293 cells, taking up to 8–10 min to achieve an apparent steady-state effect. After a washout period, T-current amplitude only partially recovered to about 55% of control level. This slow onset and incomplete washout of the effect is most likely related to the lipophilic properties of octanol and whole slice preparation vs. cultured HEK293 cells. T-current amplitude was stable for the experimental conditions shown in Fig. 3*B* (inset) for application of 30 μM octanol (n = 5) with no significant effect on the amplitude of T-current. The effect of octanol on T-current in TC neurons was concentration-dependent, yielding an IC_{50} 287 ± 15 μM (n = 22, Fig. 3*C*). In contrast to the slow onset and incomplete washout of inhibition of T-current by octanol, 10 mM nickel, the traditional T-channel blocker, rapidly and completely reversibly inhibited the T-current of TC neurons (n = 4, data not shown).

Mechanisms of inhibition of T-current in TC neurons by octanol

To investigate the mechanisms of T-current inhibition by octanol in native TC neurons, we first performed I–V experiments in control conditions (top traces on Fig. 4A) and immediately 10 minutes after application of 1mM octanol (bottom traces on Fig. 4A). For these experiments we set V_h at −70 mV in order to decrease error resulting from imperfect space clamp conditions in intact brain slice preparation. The family of elicited currents showed the typical criss-crossing pattern of T-current due to faster activation and inactivation kinetics at more positive test potentials. Averaged I–V curves illustrated on Fig. 4B indicate that octanol (open symbols) inhibited most of the peak current from control conditions (filled symbols) over the range of all tested potentials. Figure 4C and 4D show conductance curves calculated from I–V curves in the control conditions (filled symbols) and after applications of octanol (open symbols). We found that that octanol induced a significant depolarizing shift in conductance curves of about 7 mV when compared to the control.

Modulation of steady-state-inactivation of T-current in TC neurons and recombinant $Ca_V3.1$ currents by octanol

Binding to inactivated states is an important property of drugs that modulate ion channels because it can provide selectivity to their action. Transitions from closed to inactivated states can be measured using long prepulses at different potentials, producing what are commonly referred to as steady-state inactivation curves. We assessed steady-state inactivation curves using a standard double-pulse protocol with 3.5-s long prepulses to variable voltages (from −110 to −50 mV in 5-mV increments) and V_t to −50 mV in brain slices and V_t of −30 mV in HEK293 cells. Top and middle panels of Fig. 5A show summary of these experiments with recombinant $Ca_V3.1$ currents and Fig. 5B illustrates similar experiments in TC neurons in brain slices before (filled symbols) and after application of octanol (open symbols). From these

experiments, we found that octanol caused a significant hyperpolarizing shift of the steady-state relationship of about 10 mV in both native and recombinant cells. The pronounced hyperpolarizing shift in V_{50} could be essential for the resulting inhibitory effect of octanol on T-current in TC neurons. The small discrepancy in the effects of octanol on activation kinetics may be related to the differences between native and recombinant channels, and/or imperfect conditions for biophysical studies in intact TC cells.

T-channels activate and inactivate over similar membrane potentials. This property allows for a small range of potentials at which T-channels are available for activation, but have not yet fully inactivated. This phenomenon, represented by the overlapping regions of the Boltzmann curves for activation and inactivation, is referred to as window current. Using electrophysiological and computational modeling approaches, evidence of window currents has been obtained in TC neurons, where they are important in signal amplification (Williams et al., 1997; Hughes et al., 1999). Thus, we assessed whether the effects of octanol on steady-state activation and steady-state inactivation decrease window current in both HEK293 (bottom panel of Fig. 5A) and TC cells (bottom panel of Fig. 5B). These figures show overlapping curves obtained with steady-state activation and steady-state inactivation in control (solid line) and during application of octanol (dashed lines) over the broad range of membrane potentials. It is evident that octanol almost completely abolished the area under the curves representing window current.

Octanol speeds up recovery of T-current from fast inactivation in TC neurons at hyperpolarized membrane potentials

The time course of recovery from inactivation (deinactivation) in the range of few hundred milliseconds is an important property of T-type channels. LTCS are often triggered after an inhibitory postsynaptic current (IPSC), and this is due to fast recovery of T-channels during the IPSC, followed by their opening as the membranes returns to its resting potential (McCormick and Bal 1997; Perez-Reyes 2003). Since recovery rates can modulate excitability of neuronal cell with T-current expression, we investigated the effect of octanol on recovery from fast T-current inactivation. For performing these experiments, we applied double pulse protocol. TC cells were first depolarized from V_h −90 mV to V_t −50 mV for 320 milliseconds to elicit near-maximal T-current (first pulse). In a second step (recovery phase) cells were hyperpolarized for varying intervals ($V_{h\ rec}$) from 2 ms to ≥1 s and then released again to V_t −50 mV. We found that in control conditions T-current recovered somewhat faster at more hyperpolarized membrane potentials during recovery phase giving the average recovery time constant (τ) at $V_{h\ rec}$ −90 mV (± SD): 255 ± 10 ms, n = 20; and at $V_{h\ rec}$ −120 mV: 157.0 ± 13 ms, n = 8 ($p<0.001$, data not shown). Similar mild voltage-dependence of recovery from inactivation was observed in recombinant $Ca_V3.1$ currents (Serrano et al. 1999). Experiments with octanol in thalamic slices using this protocol are summarized in Figure 6A. Surprisingly, application of octanol did not slow recovery rate as would have been predicted by its effect on steady-state inactivation curves (Fig. 5*B*). Contrastingly, octanol accelerated recovery from inactivation of T-currents in TC cells by about 2 fold. As depicted with solid lines on Fig 6A, analysis with single exponential function showed significant different recovery time constants ($V_{h\ rec}$ −90 mV: control τ = 255 ± 10 ms, 1 mM octanol τ = 136 ± 7 ms, n=5, $p < 0.01$). We found similar effect at more negative recovery potentials such as $V_{h\ rec}$ −120 mV as follows: control τ = 157 ± 13 ms, 1 mM octanol τ = 44 ± 5 ms, $p < 0.01$ (n=8, data not shown). To examine if this effect of octanol on speeding of recovery from inactivation of T-currents in TC cells can be mimicked with another aliphatic alcohol, we performed similar experiments with 1 mM heptanol (Fig. 6B). Consistent with its lesser potency in recombinant cells (Fig. 1F), heptanol at 1 mM inhibited about 50% of T-current amplitude in TC cells (data not shown). However, Figure 6B shows that heptanol, very much like octanol, significantly speeded recovery from inactivation in TC cells almost 2-fold. We next examined the ability of another

class of general anesthetics and T-channel inhibitor like isoflurane to modulate recovery from inactivation in TC cells (Fig. 6C). We found that in contrast to aliphatic alcohols, isoflurane slowed recovery from inactivation of T-currents in TC cells. This slowing of recovery from inactivated states of T-channels in TC cells is in agreement with our recent study examining the effects isoflurane on kinetic properties of recombinant human $Ca_V3.1$ and $Ca_V3.2$ channels (Orestes et al., 2009). Finally, Figure 6D shows that similarly to isoflurane (Orestes et al., 2009), octanol slowed recovery form inactivation of recombinant $Ca_V3.1$ current, as evident by about 2-fold shift to the right in curves representing best fits to the average data points. Thus, it appears that the unique effect of aliphatic alcohols on recovery from inactivation of $Ca_V3.1$ T-channels is confined to the native TC cells.

Octanol inhibits LTCSs and burst firing of TC neurons

Based on our biophysical studies, we hypothesized that octanol may abolish T-channel-dependent LTCSs and associated spike firing of TC neurons more effectively at depolarized membrane potentials. Thus, we used current-clamp recordings from these cells and assessed spike firing when the neuronal membrane was transiently depolarized with direct current injections through the recording electrode. Figure 7 illustrates that we first used protocols with membrane potentials from 70–80 mV, which sufficiently increase the availability of T-channels. Figure 7A (top, middle and bottom panels) presents traces from a representative TC cell before, during, and after the application of 1 mM octanol. Octanol almost completely abolished the amplitude of LTCS and diminished number of action potentials (APs) that crowned LTCS from 8 to 0. The top histogram in Figure 7B indicate that in similar current-clamp experiments 1 mM octanol significantly decreased the membrane firing that accompanied LTCS from an average of about 6 to 1 APs ($n = 5$ cells, $p < 0.001$). In contrast, applications of octanol had variable effects on passive membrane properties of these neurons. However, in average octanol did not significantly affect passive membrane properties of TC neurons ($n = 7$) like resting membrane potential (RMP) as presented on middle panel of Fig. 7B, and input resistance (R_{in}) as depicted on histogram on the bottom panel of Fig. 7B. Next, we designed the protocol where LTCSs and rebound spike firing were evoked by prior hyperpolariziation of neuronal membrane by injecting hyperpolarizing pulses of escalating amplitudes *via* recording electrode (constant 450 ms duration and in 50 pA increments) as depicted on top traces of Figure 8. It is well established that rebound spike firing under these conditions is critically dependent on recovery from inactivation of T-channels in TC cells (Llinas et al., 1988; McCormick and Ball, 1997;Kim et al., 2001;Steriade, 2005). Traces on the left of Figure 8 show rebound spike firing of a representative TC cell in control conditions and traces on the right are from the same cell after > 6 minutes of application of 1 mM octanol. Initially, octanol completely abolished rebound spike firing at membrane potentials of −87 mV and −90 mV, while spike firing partially recovered with progressive hyperpolarizations of neuronal membrane to −97 mV and −117 mV (two bottom traces on the right of Fig. 8). We demonstrated similar effects of octanol using the same current-clamp protocol in 2 other TC cells (data not shown). Thus, it appears that due to its voltage-dependent block and contrasting effects on recovery from T-current inactivation, octanol is more effective in suppressing neuronal excitability of TC cells at more depolarized membrane potentials. However, it should be noted that the effects of octanol on other voltage-gated currents that control excitability in these cells may have also contributed to its effect on membrane firing.

DISCUSSION

Even though inhibitory effect of octanol on native T-current in brain stem slice preparation was reported more than two decades ago (Llinas, 1988), the underlying biophysical mechanism of this inhibition and its possible relevance to the pharmacological effects of octanol have not been well studied. The major finding of our present study is that octanol voltage-dependently

inhibits recombinant human $Ca_V3.1$ and native T-type currents in rat TC relay neurons, with more potent inhibition occurring at depolarized membrane potentials. We also found that other anesthetic alcohols with shorter number of carbon atoms like heptanol and hexanol were less potent in inhibiting recombinant $Ca_V3.1$ currents. Similar order of potency of anesthetic alcohols was noted for the inhibition of recombinant voltage-gated Na^+ channels (Horishita and Harris, 2008). Interestingly, anesthetic capacity of aliphatic alcohols in animal models such as tadpole assay of loss of righting reflex (LORR) also decreases with of shorter chain molecules (Alifimoff et al., 1989). This argues that both pharmacological effects such as hypnosis and interactions of anesthetic alcohols with potential cellular targets such as voltage-gated ion channels require structural specificity.

The conclusion that a drug at relevant concentrations blocks any relevant ion channel *in vitro* is usually based on comparisons of the apparent IC_{50} for block observed *in vitro* with the plasma concentrations reached *in vivo*. To our knowledge, no such information is currently available for octanol in mammals. However, it has been reported that aliphatic alcohols have anesthetic properties *in vivo* measured with LORR with the estimated aqueous concentration in tadpoles ranging from 57–130 μM, 230–350 μM and 570–900 μM for octanol, heptanol and hexanol, respectivelly (Alifimoff et al., 1989). Assuming that similar concentrations occur in mammalian brains during general anesthesia, it appears that T-channels are only partially inhibited by relevant concentrations of octanol and other aliphatic alcohols (likely 20 %−40 % inhibition at physiological membrane potentials). However, since T-channels are a critically determining threshold for Na^+ channels that fire in an all-or-nothing manner, one can argue that even partial inhibition of thalamic T-current with clinically used drugs may have a pronounced effect on membrane firing and low-frequency pacemaker oscillations (e.g. anticonvulsant ethosuximide; Huguenard and Prince, 1994). Consistent with this idea, current-clamp experiments in TC cells in brain slices from guinea pigs and cats have shown that the application of 50 μM octanol (Puil et al., 1994), and 50–100 μM octanol (Soltesz et al., 1991) blocked T-channel-dependent LTCS and underlying low-frequency oscillations, respectively. Furthermore, we reported recently that octanol at 10 μM inhibited T-currents and LTCS in the rat reticular thalamic (nRT) neurons in slices (Joksovic et al., 2010). However, as discussed earlier, it is likely that actual concentrations of lipophilic drugs such as anesthetics in brain slices are much lower than their nominal concentrations. Based on this, we hypothesized that the inhibitory effect of octanol on T-channel-dependent LTCSs and neuronal burst firing could at least contribute to the inhibitory effect of aliphatic alcohols on sensory processing in the thalamocortical pathway *in vivo*..

Our data from this study with native TC cells are in agreement with our previous finding that octanol inhibits recombinant rat $Ca_V3.1$ and human $Ca_V3.2$ currents with respective IC_{50} values of 160 μM and 220 μM (Todorovic et al., 2000). However, it should be noted that at these concentrations potentiation of inhibitory current mediated by $GABA_A$ channels (Franks and Lieb, 1994) and inhibition of currents through voltage-gated Na^+ channels (Horishita and Harris, 2008) have also been reported. Thus, it is likely that state-dependent inhibition of T-currents, in concert with the effects of octanol on other currents, may inhibit the neuronal excitability underlying functional states of TC cells and consequently inhibit thalamo-cortical information transfer.

In this and our recent study (Joksovic et al., 2010) octanol exhibited voltage-dependent features of channel inhibition in both native and recombinant cells expressing different T-type current variants. This was also well documented for different voltage-dependent blockers of T-type channels such as isoflurane (Orestes et al., 2009) and arachidonic acid (Talavera et al., 2004), which inhibit recombinant $Ca_V3.1$ currents. This is important since inhibitory effects of these drugs are consequently more prominent at depolarized membrane potentials that could occur during awake states and less prominent at hyperpolarized membrane potentials such as those

which dominate during sleep states thought to be initiated upon activation of nRT neurons that provide inhibitory postsynaptic potentials (IPSPs) to TC cells.

One particularly interesting aspect of our study is that octanol preferentially inhibited T-channels in inactive states, yet increased the rate of recovery from inactivation. This is in contrast with a current concept that a drug that stabilizes inactive states of the channel is usually slowing its recovery from inactivation since it takes longer for drug to dissociate from the channel. The current kinetic models often assume the existence of a pool of several linearly interconnected inactivated states (e.g. Serrano et al., 1999; Burgess et al., 2002; Talavera et al., 2004). According to this model, voltage-dependent blockers would cause the channels to accumulate in more remote inactivated states which would be evident as a hyperpolarizing shift in steady-state inactivation curves. As a consequence, recovery rates would become slower in the presence of voltage-dependent blockers, because recovery from remote inactivated states requires a transition through a higher number of intermediate inactivated states. Indeed, this was well documented for different voltage-dependent blockers of T-channels such as isoflurane (Orestes et al. 2009) and arachidonic acid (Talavera et al. 2004) in inhibiting recombinant $Ca_V3.1$ currents. However, our data suggest that in the case of inhibition of native T-currents in TC cells but not recombinant human $Ca_V3.1$ currents, octanol may promote an additional alternate pathway for recovery from inactivated states that is facilitated with stronger membrane hyperpolarizations. It is unlikely that this finding could be related to imperfect space-clamp in brain slices since it is mimicked by another aliphatic alcohol such as heptanol but not by different class of anesthetics such as isoflurane (Fig. 6). This argues that the effect of octanol on speeding of recovery from inactivated states of T-currents in TC cells is agent-specific. While this mechanism of current inhibition has not been described previously for T-channels, similar finding was reported for voltage-gated Na^+ and voltage-gated K^+ channels. Specifically, Mullins et al. (2002) presented a model where both hastening of recovery from inactivation of hERG K^+ channels and accelerated entry into inactivated states are induced by Na^+ ions. Similarly, Szendroedi et al. (2007) reported that Cd^{2+} ions blocked currents though recombinant voltage-gated Na^+ channels by shifting steady-state inactivation to hyperpolarized potentials and concomitantly speeding the recovery from inactivation. They further proposed that such effect could be mediated by binding of the drug to the selectivity filter region which could act as “foot-on-the-door” promoting the channel to close and at the same time increasing the rate of recovery from inactivation. It is possible that the effects of aliphatic alcohols on recovery form inactivation in native TC cells could be related to the presence of endogenous molecules, differences between rat and human channels, and/or alternative splice variants of $Ca_V3.1$ that can modulate T-channel function. For example, native T-channels in rat TC cells undergo unique regulation of inactivation with ATP to allow paradoxical potentiation of T-current at depolarized membrane potentials (Leresche et al., 2004). Furthermore, alternative splicing of $Ca_V3.1$ has been described (Mittman et al., 1999; Monteil et al., 2000) and may give rise to different properties of channel gating and inactivation (Chemin et al., 2001). Importantly, molecular studies have suggested that multiple splice variants of $Ca_V3.1$ may exist in rat TC cells based on variations encompassing exons 25 and 26 (Broicher et al., 2007). However, the extent of contribution of each splice variant to native T-current in TC cells is not known. Further extensive molecular, biophysical and modeling studies will be needed to elucidate whether similar mechanisms or other post-translational modifications of $Ca_V3.1$ may underlay the effects of octanol and other aliphatic alcohols on recovery from inactivation of T-channels in TC neurons.

In conclusion, we have examined the sensitivities of recombinant $Ca_V3.1$ and native TC T-currents to various aliphatic alcohols. Our results indicate that in spite of similar pharmacological sensitivities and voltage-dependent inhibition, aliphatic alcohols had contrasting effects on recovery from inactivation of native and recombinant currents.

Furthermore, the effects of aliphatic alcohols on these currents may contribute to their pharmacological effects.

Acknowledgments

The authors thank FAI Materials Testing Laboratory (Marietta, GA) for concentration measurements of dissolved octanol. We also thank Professor Eberhard Kochs, Department of Anesthesiology, Klinikum rechts der Isar and Technische Universität München, Munich, Germany for support of V.-S. Eckle. We thank Dr. Edward Perez-Reyes for providing us with recombinant HEK293 cells with stably expressed $Ca_V3.1$ channels and Dr. Peihan Orestes for help with cell cultures.

This work was supported by National Institute of Health Grant GM-070726 to S. M. Todorovic.

REFERENCES

Alifimoff JK, Firestone LL, Miller KW. Anaesthetic potencies of primary alkanols: implications for the molecular dimensions of the anaesthetic site. Br. J. Pharmacol 1989;96:9–16. [PubMed: 2784337]

Alkire MT, Haier RJ, Fallon JH. Toward a unified theory of narcosis: brain imaging evidence for a thalamocortical switch as the neurophysiologic basis of anesthetic-induced unconsciousness. Conscious. Cogn 2000;9:370–386. [PubMed: 10993665]

Angel A. Adventures in anesthesia. Exp. Physiol 1991;76:1–38. [PubMed: 2015066]

Burgess DE, Crawford O, Delisle BP, Satin J. Mechanism of inactivation gating of human T-type (low-voltage-activated) calcium channels. Biophys. J 2002;82:1894–1906. [PubMed: 11916848]

Broicher T, Kanyshkova T, Landgraf P, Rankovic V, Meuth P, Meuth SG, Pape HC, Budde T. Specific expression of low-voltage-activated calcium channel isoforms and splice variants in thalamic local circuit interneurons. Mol. Cell. Neurosci 2007;36(2):132–145. [PubMed: 17707654]

Chemin J, Monteil A, Bourinet E, Nargeot J, Lory P. Alternatively spliced alpha(1G) (Ca(V)3.1) intracellular loops promote specific T-type Ca(2+) channel gating properties. Biophys. J. 2001 2001;80 (3):1238–1250.

Chesney MA, Perouansky M, Pearce RA. Differential uptake of volatile agents into brain tissue in vitro. Measurement and application of a diffusion model to determine concentration profiles in brain slices. Anesthesiology 2003;99:122–130. [PubMed: 12826851]

Franks NP, Lieb WR. Molecular and cellular mechanisms of general anesthesia. Nature 1994;367:607–614. [PubMed: 7509043]

Franks NP. General anaesthesia: from molecular targets to neuronal pathways of sleep and arousal. Nat. Rev. Neurosci 2008;9:370–386. [PubMed: 18425091]

Herrington J, Lingle CJ. Kinetic and pharmacological properties of low-voltage-activated Ca^{2+} current in rat clonal (GH3) pituitary cells. J. Neurophysiol 1992;68:213–232. [PubMed: 1325546]

Horishita T, Harris RA. N-alcohols inhibit voltage-gated Na^+ channels expressed in Xenopus oocytes. JPET 2008;326:270–277.

Hughes SW, Cope DW, Toth TI, Williams SR, Crunelli V. All thalamocortical neurones possess a T-type Ca2+ 'window' current that enables the expression of bistability-mediated activities. J. Physiol 1999;517:805–815. [PubMed: 10358120]

Huguenard JR, Prince DA. Intrathalamic rhythmicity studied in vitro: nominal T-current modulation causes robust antioscillatory effects. J. Neurosci 1994;14:5485–5502. [PubMed: 8083749]

Joksovic PM, Bayliss DA, Todorovic SM. Different kinetic properties of two T-type Ca^{2+} currents of rat reticular thalamic neurons and their modulation by enflurane. J. Physiol 2005;566:125–142. [PubMed: 15845580]

Joksovic PM, Choe W, Nelson MT, Orestes P, Brimelow BC, Todorovic SM. Mechanisms of inhibition of T-type calcium current in the reticular thalamic neurons by 1-octanol: implication of the protein kinase C pathway. Mol. Pharmacol 2010;77(1):87–94. [PubMed: 19846748]

Joksovic PM, Nelson MT, Jevtovic-Todorovic V, Patel MK, Perez-Reyes E, Campbell KP, Chen C-C, Todorovic SM. $Ca_V3.2$ (α1H) channel is the major molecular substrate for redox regulation of T-type channels in the rat and mouse thalamus. J. Physiol. (London) 2006;574(Pt 2):415–430. [PubMed: 16644797]

Kim D, Song I, Keum S, Lee T, Jeong M-J, Kim S-S, McEnery MW, Shin H-S. Lack of the burst firing of thalamocortical relay neurons and resistance to absence seizures in mice lacking α_{1G} T-type Ca^{2+} channels. Neuron 2001;31:35–45. [PubMed: 11498049]

Leresche N, Hering J, Lambert RC. Paradoxical potentiation of neuronal T-type Ca2+ current by ATP at resting membrane potential. J. Neurosci 2004;16(24):5592–5602. [PubMed: 15201332]

Llinás RR. The intrinsic electrophysiological properties of mammalian neurons: insights into central nervous system function. Science 1988;242:1654–1664. [PubMed: 3059497]

Llinás RR, Choi S, Urbano FJ, Shin HS. Gamma-band deficiency and abnormal thalamocortical activity in P/Q-type channel mutant mice. Proc. Natl. Acad. Sci. U S A 2007;104:17819–17824. [PubMed: 17968008]

Llinas RR, Ribary U, Jeanmonod D, Kronberg E, Mitra PP. Thalamocortical dysrhythmia: A neurological and neuropsychiatric syndrome characterized by magnetoencephalography. Proc. Natl. Acad. Sci. U S A 1998;96:15222–15227. [PubMed: 10611366]

McCormick DA, Bal T. Sleep and arousal: thalamocortical mechanisms. Annu. Rev. Neurosci 1997;20:185–215. [PubMed: 9056712]

Mittman S, Guo J, Agnew WS. Structure and alternative splicing of the gene encoding alpha1G, a human brain T calcium channel alpha1 subunit. Neurosci. Lett 1999;274(3):143–146. [PubMed: 10548410]

Monteil A, Chemin J, Bourinet E, Mennessier G, Lory P, Nargeot J. Molecular and functional properties of the human α1G subunit that forms T-type calcium channels. J. Biol. Chem 2000;275:6090–6100. [PubMed: 10692398]

Mullins FM, Stepanovic SZ, Desai RR, George AL Jr, Balser JR. Extracellular sodium interacts with the HERG channel at an outer pore site. J. Gen. Physiol 2002;120:517–537. [PubMed: 12356854]

Orestes P, Bojadzic D, Chow RM, Todorovic SM. Mechanisms and functional significance of inhibition of neuronal T-type calcium channels by isoflurane. Mol. Pharmacol 2009;75:542–554. [PubMed: 19038845]

Perez-Reyes E. Molecular physiology of low-voltage-activated T-type calcium channels. Physiol. Rev 2003;83:117–161. [PubMed: 12506128]

Puil E, Meiri H, Yarom Y. Resonant behavior and frequency preferences of thalamic neurons. J. Neurophysiol 1994;71:575–582. [PubMed: 8176426]

Serrano JR, Perez-Reyes E, Jones SW. State-dependent inactivation of the α1G T-type calcium channel. J. Gen. Physiol 1999;114:185–201. [PubMed: 10435997]

Sherman SM. Thalamic relays and cortical functioning. Prog. Brain. Res 2005;149:107–126. [PubMed: 16226580]

Soltesz I, Lightowler S, Leresche N, Jassik-Gerschenfeld D, Pollard CE, Crunelli V. Two inward currents and the transformation of low-frequency oscillations of rat and cat thalamocortical cells. J. Physiol 1991;441:175–197. [PubMed: 1667794]

Swanson, LW. Brain maps: Structure of the rat brain. Amsterdam: Elsevier; 1992.

Steriade M. Sleep, epilepsy and thalamic reticular inhibitory neurons. TINS 2005;28:317–324. [PubMed: 15927688]

Szendroedi J, Sandtner W, Zarrabi T, Zebedin E, Hilber K, Dudley SC Jr, Fozzard HA, Todt H. Speeding the recovery from ultraslow inactivation of voltage-gated Na+ channels by metal ion binding to the selectivity filter: a foot-on-the-door? Biophys. J 2007;93:4209–4224. [PubMed: 17720727]

Takahashi K, Wakamori M, Akaike N. Hippocampal CA1 pyramidal cells of rats have four voltage-dependent calcium conductances. Neurosci. Lett 1989;104:229–234. [PubMed: 2554221]

Takenoshita M, Steinbach JH. Halothane blocks low-voltage-activated calcium current in rat sensory neurons. J. Neurosci 1991;11:1404–1412. [PubMed: 1851220]

Talavera K, Staes M, Janssens A, Droogmans G, Nilius B. Mechanism of arachidonic acid modulation of the T-type Ca2+ channel alpha1G. J. Gen. Physiol 2004;124:225–238. [PubMed: 15314070]

Talley EM, Cribbs LL, Lee J, Daud A Perez-Reyes E, Bayliss DA. Differential distribution of three members of a gene family encoding low-voltage-activated (T-type) calcium channels. J. Neurosci 1999;19:1895–1911. [PubMed: 10066243]

Todorovic SM, Lingle CJ. Pharmacological properties of T-type Ca2+ current in adult rat sensory neurons: effects of anticonvulsant and anesthetic agents. J. Neurophysiol 1998;79:240–252. [PubMed: 9425195]

Todorovic SM, Perez-Reyes E, Lingle CJ. Anticonvulsants but not general anesthetics have differential blocking effects on different T-type current variants. Mol. Pharmacol 2000;58:98–108. [PubMed: 10860931]

Williams SR, Toth TI, Turner JP, Hughes SW, Crunelli V. The 'window' component of the low threshold Ca2+ current produces input signal amplification and bistability in cat and rat thalamocortical neurones. J. Physiol 1997;505:689–705. [PubMed: 9457646]

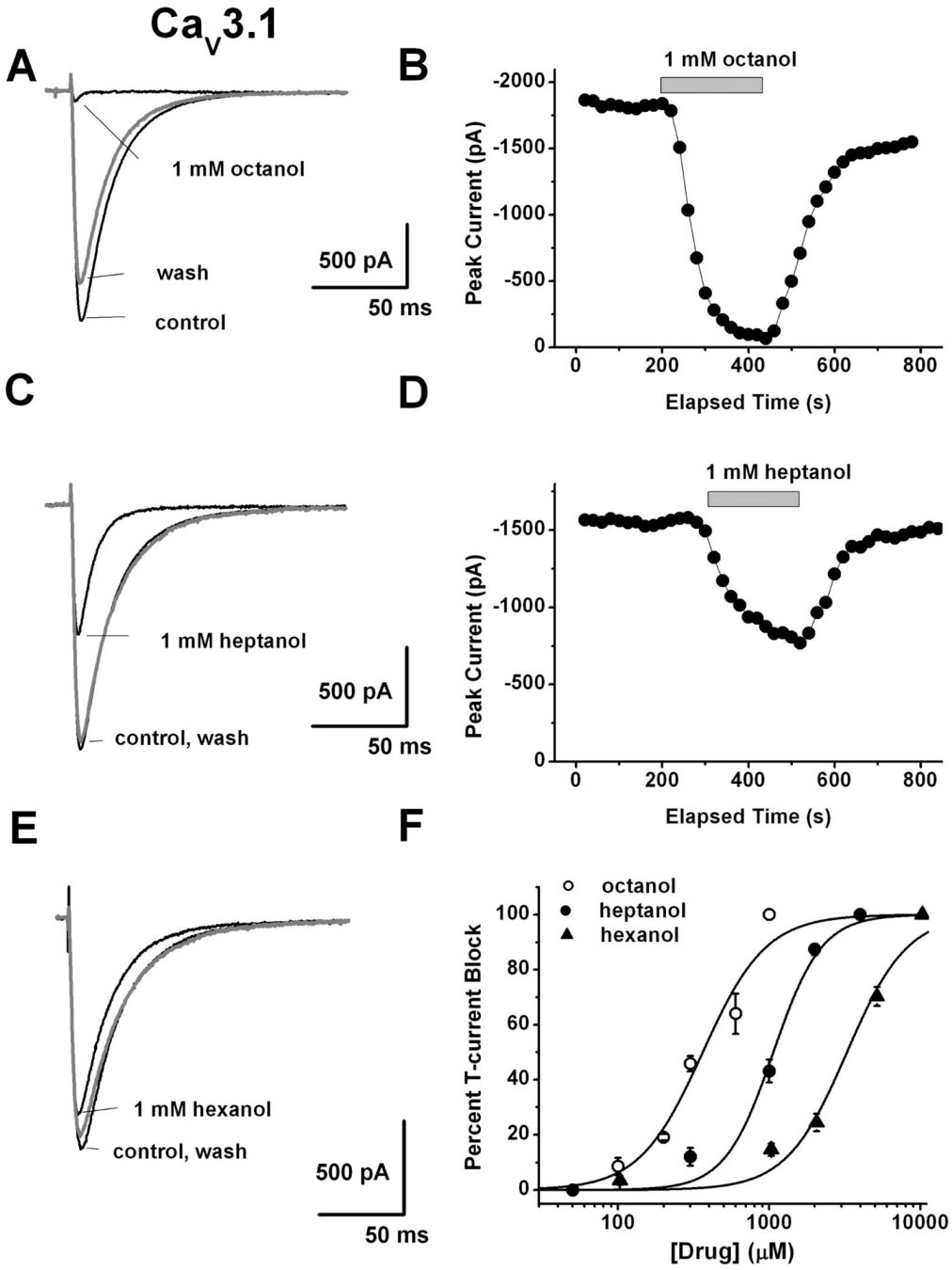

Figure 1. Concentration-dependent inhibition of recombinant human Ca$_V$3.1 currents by representative aliphatic alcohols

A: Representative traces before (control), during, and after (wash) application of 1 mM octanol on HEK293 cells stably expressing Ca$_V$3.1 channels. **B**: Time course from the same cells presented on panel A of this figure showing fast and almost complete reversible inhibition of peak T-current by octanol achieved within < 2 minutes of drug application. **C**: Black traces indicate T-current before (control) and during, and gray trace depicts T-current after (wash) application of 1 mM heptanol in a representative HEK293 cell stably expressing Ca$_V$3.1 channels. **D**: Time course from the same cells presented on panel C of this figure showing stable baseline T-current amplitudes, fast and almost completely reversible inhibition of about

50% peak T-current by heptanol. **E:** Black traces indicate T-current before (control) and during, and gray trace depicts T-current after (wash) application of 1 mM hexanol in a representative HEK293 cell stably expressing $Ca_V3.1$ channels. Note that at this concentration hexanol had minimal effect on peak T-current. **F**: This panel summarizes average percent inhibition by multiple concentrations of aliphatic alcohols for octanol (open circles), heptanol (solid circles) and hexanol (solid triangles). Solid lines are best fits of data points using Hill's equation yielding IC_{50} and slope (n) values as follows for octanol (362±44 μM, n=2.1±0.5, 26 cells), for heptanol (1063±83 μM, n=2.7±0.6, 29 cells) and for hexanol (3167±329 μM, n=2.2±0.4, 27 cells). All fits are constrained to 100% maximal inhibition.

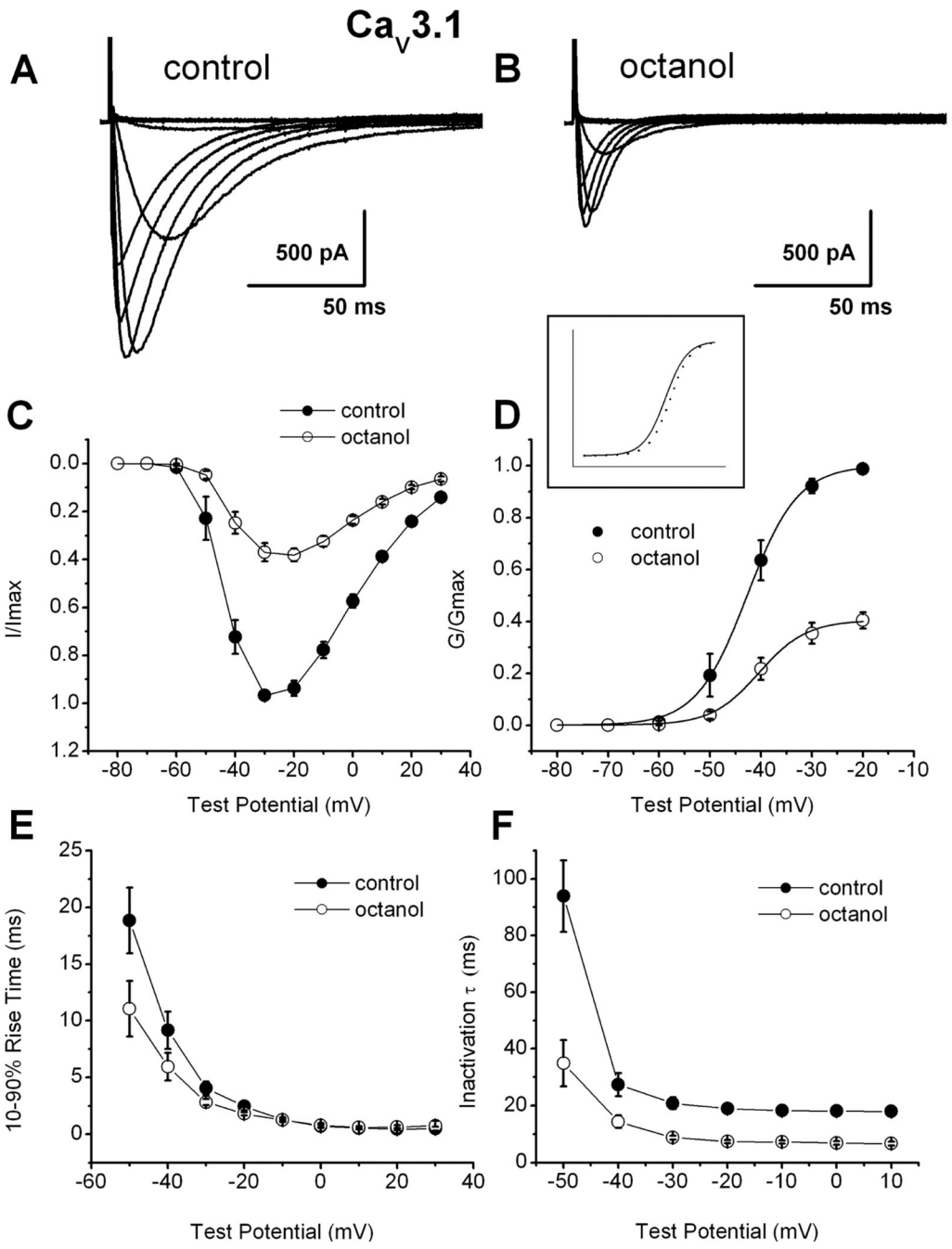

Figure 2. Mechanisms of recombinant Ca$_V$3.1 current inhibition by octanol

A: Traces of inward Ca^{2+} current in a representative HEK293 cell stably expressing human Ca$_V$3.1 constructs in control conditions (V_h −90 mV, V_t from −80 through 30 mV in 10 mV increments). **B**: Traces from the same cell using the identical voltage-protocol are obtained during an apparent steady-state inhibition of current by 1 mM octanol. **C**: The data points indicate average I–V relationships before (●) and during (○) the application of 1 mM octanol with vertical bars indicating standard errors of the mean. Currents were elicited by progressing from −80 mV to 30 mV in 10-mV increments from a holding potential of −90 mV (n = 7 cells). Note the depression of the current amplitude at most potentials in the presence of octanol. **D.** Average conductance and normalized conductance (inset) in whole-cell recordings from I–V

experiments depicted in panel C of this figure. The average half-conductance (V_{50}) was in control −42.7 ± 0.2 mV (k = 5.0 ± 0.1 mV) and in the presence of octanol was −40.4 ± 0.3 mV (k = 4.7 ± 0.3 mV). Fits were done using the Boltzmann equation. The estimated reversal potential was taken to be 50 mV. **E**: All points represent averages (n = 7 cells) of 10–90 rise time of the same cells in the control conditions (solid circles) and in the presence of octanol (open circles). Rise time was measured as time between 10% and 90% of peak current. Calculated values were significant for the V_t points of −50, −40 and 30 mV. For example, at V_t −30 mV rise times were as follows: control, 4.0±0.6; octanol, 2.8±0.3; ($p<0.01$). **F**: Rates of macroscopic current inactivation in the same cells (n = 7, error bars represent SEM) from the same cells used to generate current-voltage curves depicted in Figures 2A and 2B in control (filled symbols) and during application of 1 mM octanol (open symbols) for recombinant $Ca_V3.1$ currents. All points represent averages from multiple cells where inactivation τ was obtained at indicated potentials by fitting the decaying portion of the current with a single exponential function ($p<0.01$ at all tested points). For example, at V_t −30 mV inactivation τs were as follows: control, 20.8±2.0; octanol, 8.8±0.7; ($p<0.001$).

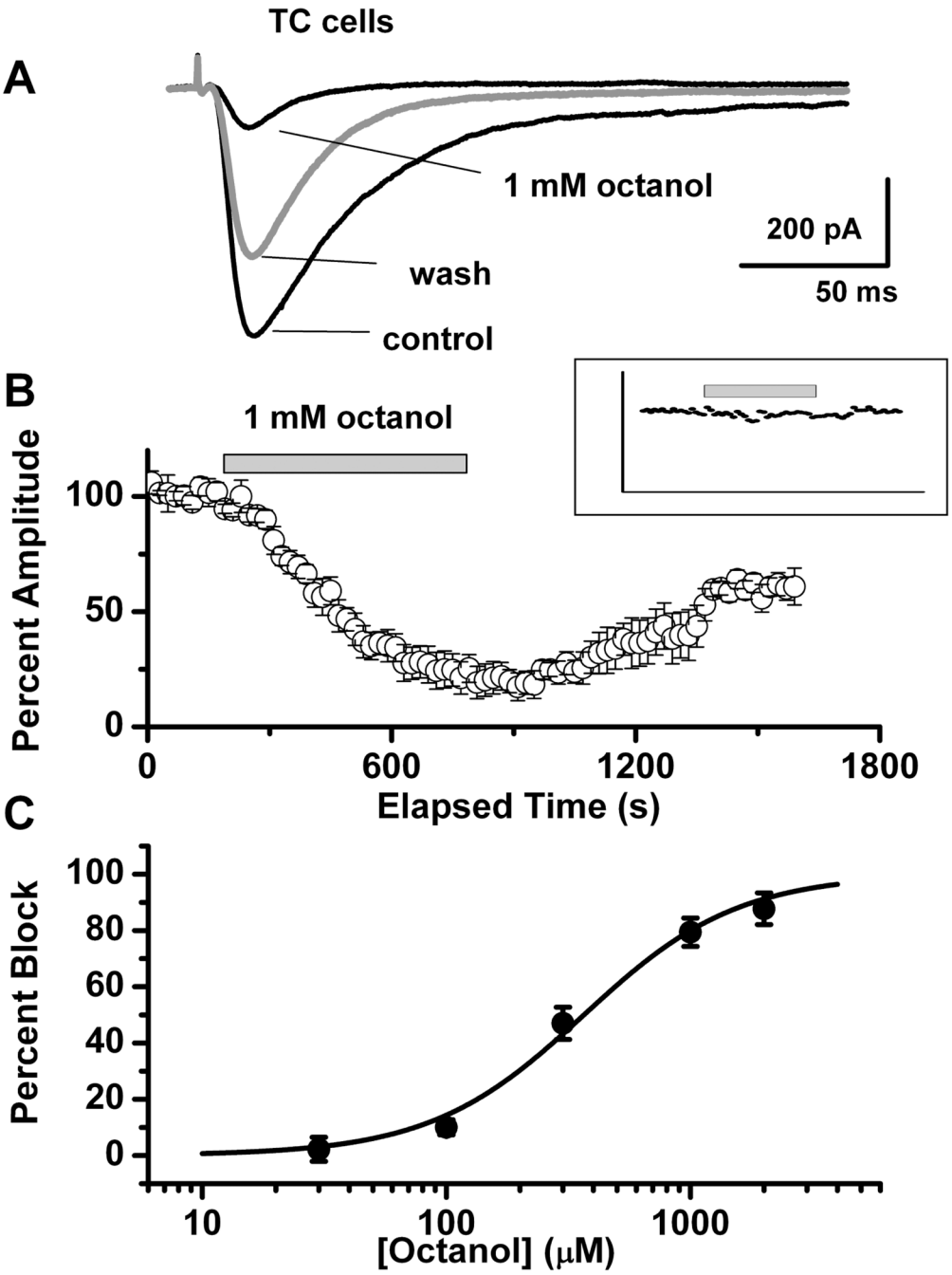

Figure 3. Inhibitory effects of octanol on T-currents in TC neurons

A: Representative traces of inward currents in a TC neuron for control, 1 mM octanol, and washout in response to voltage steps from V_h of −100 mV to V_t −50 mV. **B**: Normalized peak amplitude (averaged data from 5 cells) is plotted against the time course, showing 10 min-long application of 1 mM octanol (horizontal bar) and consecutive washout. After washout, T-current reached only about 55% of control level. Inset: Same protocol (n = 5 cells) for application of 30 μM octanol (horizontal bar). Note stable current amplitudes during applications of octanol. For clarity, error bars have been omitted. **C**: Concentration-response relationship between percentage of peak current inhibition and escalating concentrations of octanol. Averaged data points (n = 22) were fitted with a Hill equation, giving an IC_{50} = 287

± 15 μM, slope = 1.84 ± 0.16, and nearly complete (90%) maximal current inhibition. For each concentration, statistical analysis was done separately: 30 μM octanol: 2.2 ± 4.3% inhibition, $p = 0.25$; 100 μM octanol: 10.0 ± 2.7%, $p < 0.05$; 300 μM octanol: 47.0 ± 5.7%, $p < 0.0001$; 1,000 μM octanol: 79.4 ± 5.0%, $p < 0.0001$; 2,000 μM octanol: 87.7 ± 5.6%, $p < 0.0001$.

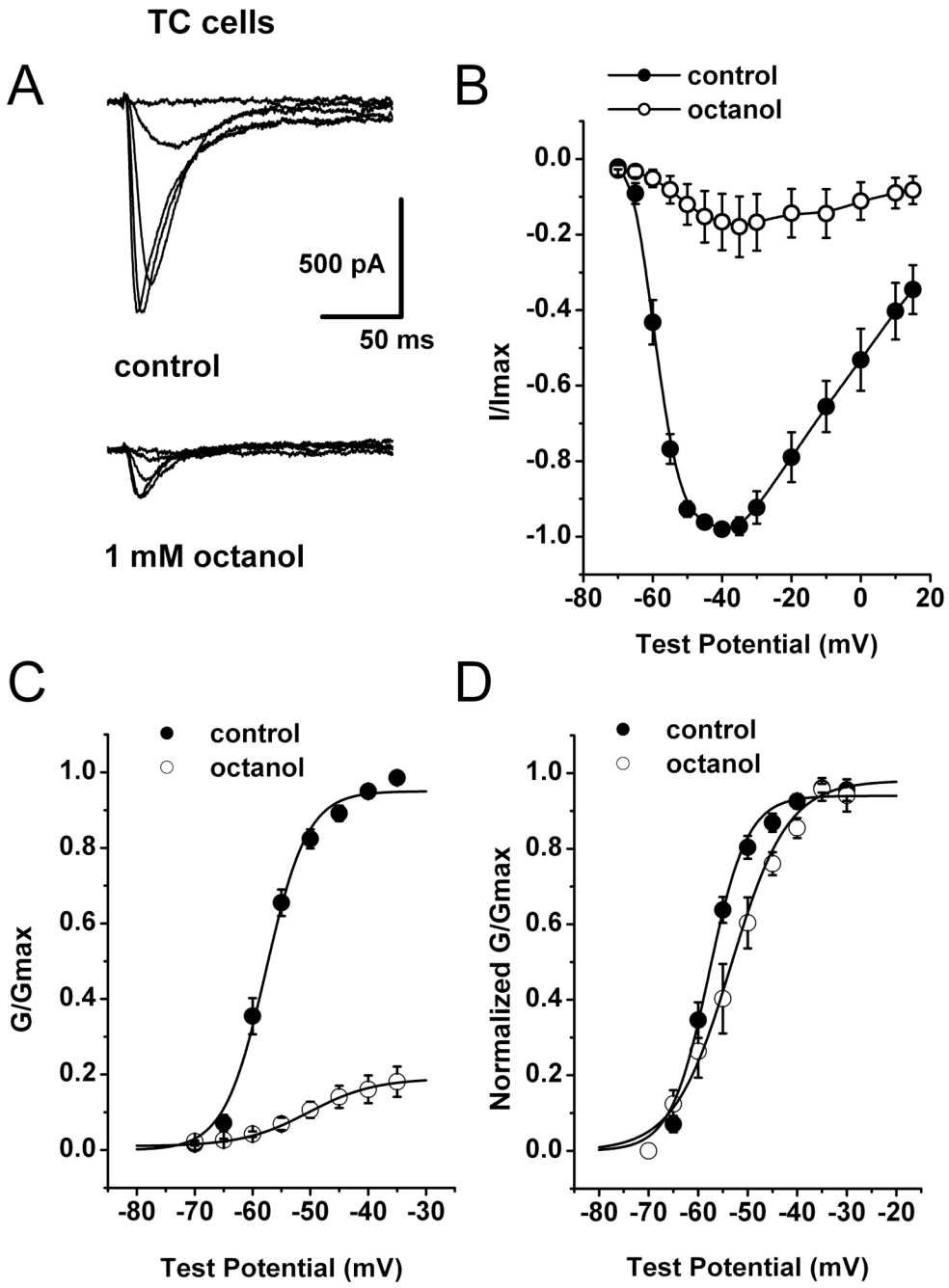

Figure 4. Mechanisms of native $Ca_V3.1$ current inhibition by octanol

A: Families of inward Ca^{2+} current traces from I–V series from a representative TC neuron. Cell was held at −70 mV, with steps ranging from −65 to −45 mV before (control, top traces) and after 10-min application of 1 mM octanol *(*bottom traces*)*. **B**: Average I–V relationships (n = 5) for control conditions (●) and after applying 1 mM octanol (○) at V_h −70 mV and V_t ranging from −70 through 15 mV in 5 mV increments. Vertical lines represent SEM and are visible only if larger than symbols. **C**: Apparent peak conductance values calculated from I–V curves and plotted against command potentials. Data points (n = 5) were normalized to the peak current elicited (G/G_{max}) under control conditions (●). Average conductance after 10 min of 1 mM octanol application is represented by open symbols (**O**). The extrapolated reversal

potential (E_r) was taken to be +55 mV. Data were fitted with a Boltzmann equation (solid lines). Vertical lines represent SEM and are visible only if larger than symbols. **D**: For easier comparison, the same data from panel C of this figure were normalized to the peak current (G/G_{max}) for the control and octanol groups. Octanol shifted activation of the channels to more depolarized potentials; V_{50}: control = −57.7 ± 0.5 mV, octanol = −50.3 ± 0.4 mV, $p < 0.05$; k: control = 3.6 ± 0.4, octanol = 5.7 ± 0.4.

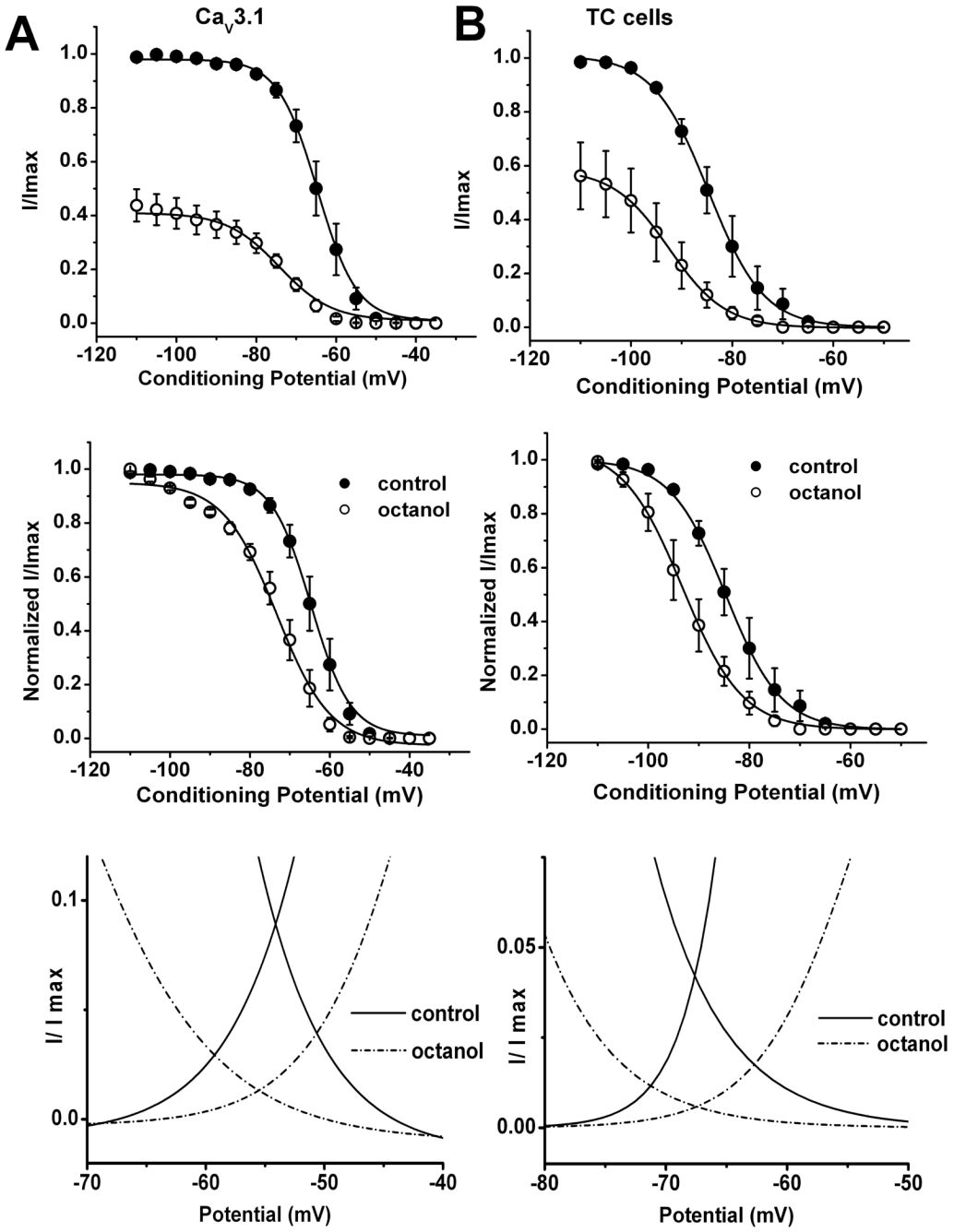

Figure 5. Similar effects of octanol on steady-state inactivation properties of T-currents in TC neurons and recombinant $Ca_V3.1$ currents

A–B: Octanol's effect on voltage-dependent steady-state inactivation in HEK293 cells (**A**) and thalamic slices (**B**). Inactivation kinetics were measured in response to a series of depolarizing command potentials from −110 mV to −50 mV, held for 3.5 sec, then stepping to −50 mV in brain slices or −30 mV in HEK293 cells. For experiments in brain slices we used 1 mM octanol that was applied for 10 minutes, for experiments in HEK293 cells 300 μM octanol was applied for 3 minutes. Top panel show average data points from these experiments with currents elicited at each command potential were normalized to the peak current elicited (I/I_{max}) for control conditions and middle panels show the same data normalized to each control conditions (filled

symbols) and octanol applications (open symbols), and plotted against the command potentials. The averaged data (n = 5) were fitted with a Boltzmann function yielding in brain slices V_{50}: control = −84.7 ± 0.2 mV, octanol = −93.2 ± 0.2 mV, $p < 0.05$; k: control = 5.46 ± 0.2, octanol = 5.94 ± 0.2. In recombinant HEK293 cells expressing $Ca_V3.1$ channels (n = 6) we obtained the following results: V_{50}: control = −64.7 ± 0.2 mV, octanol = −73.3 ± 0.6 mV, $p < 0.001$; k: control = 4.9 ± 0.2, octanol = 6.7 ± 0.6.

Bottom panels on this figure show window T-current of recombinant $Ca_V3.1$ current (on the left) and native T-current sin TC neurons (on the right) consisting of steady-state inactivation curves and activation curves for control (solid lines) and octanol (dashed lines) groups.

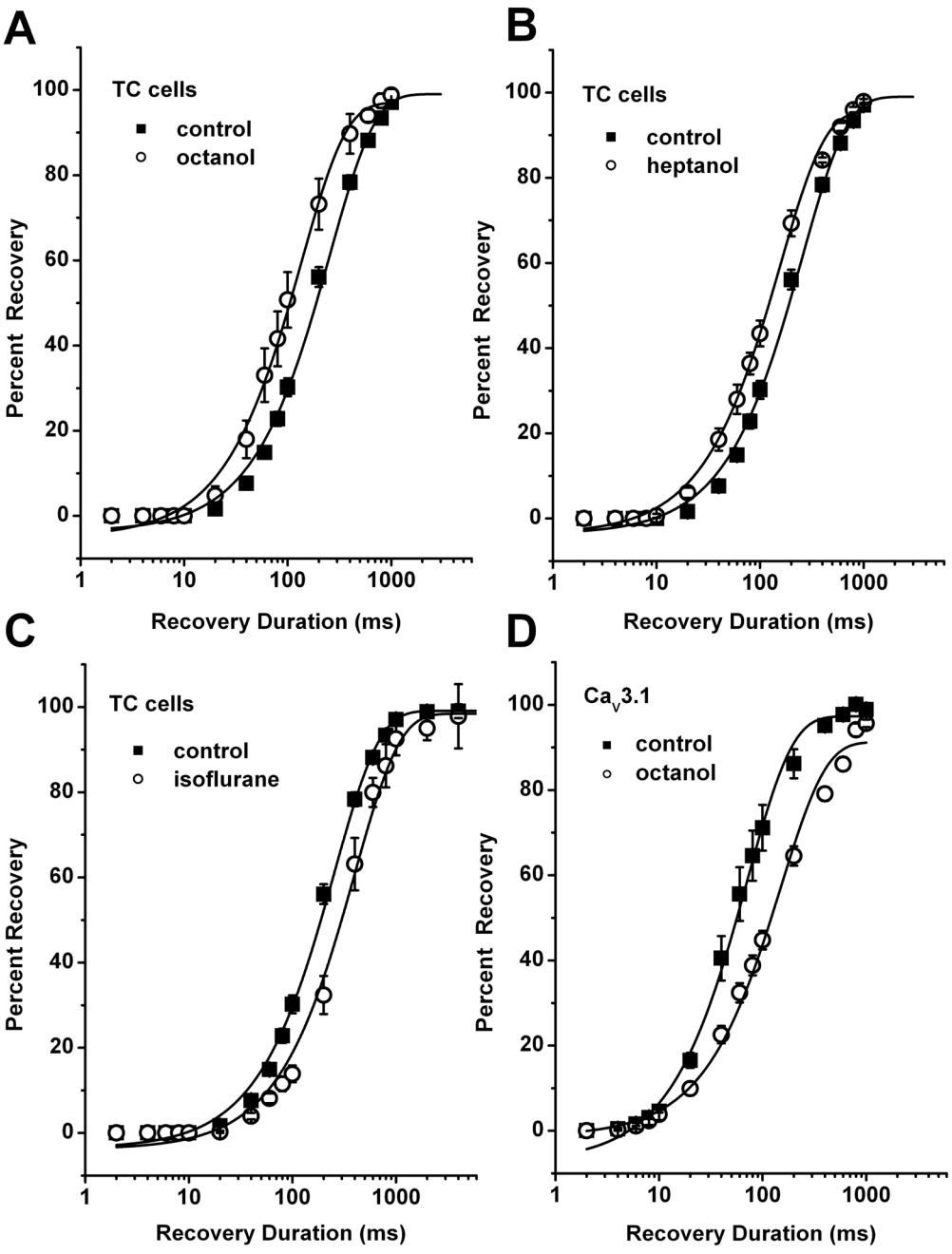

Figure 6. Contrasting effects of aliphatic alcohols and isoflurane on T-current deinactivation in TC neurons

A–D: Double pulse protocol was used to generate average data points from multiple experiments as outlined in the text. Filled square symbols are obtained in control conditions before drug application (for panels A–C controls are pulled together, $V_{h\ rec}$ −90 mV: control τ= 255 ± 10 ms,). Drugs (open symbols) are applied for at least 10 minutes in brain slices (A–C) and for at least 3 minutes in the experiments with HEK293 cells expressing stable $Ca_V3.1$ constructs (panel D). Solid lines are best fits using single-exponential function (see Materials and Methods). Note that octanol (panel A, 1 mM octanol τ = 136 ± 7 ms, n=5, $p < 0.01$) and heptanol (panel B, 1 mM heptanol τ = 159 ± 6 ms, n=5, $p < 0.01$) similarly increased the rate

of recovery from inactivation of T-currents in TC cells as evident by leftward shift in average recovery duration. In contrast, isoflurane under identical recording conditions shifted average recovery duration to the right (panel C, $V_{h\ rec}$ −90 mV: 2% isoflurane $\tau = 399 \pm 23$ ms, n=5, $p < 0.001$)). Octanol in recombinant HEK293 cells expressing $Ca_V3.1$ channels induced slowing of recovery from inactivation for about 2-fold (panel D, $V_{h\ rec}$ −90 mV: control $\tau = 71 \pm 3$ ms, 0.6 mM octanol $\tau = 150 \pm 10$ ms, n=5, $p < 0.001$).

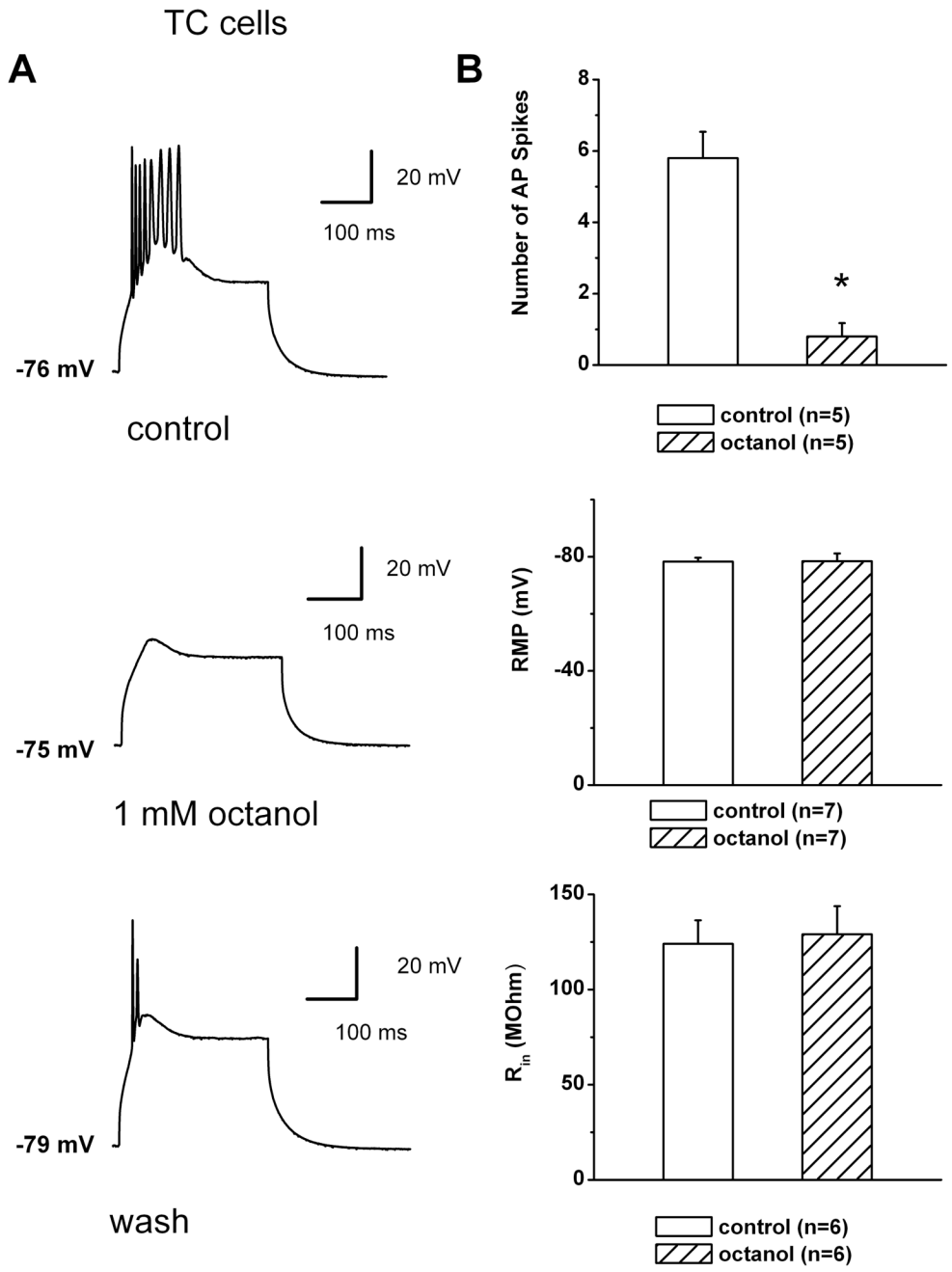

Figure 7. Octanol inhibits burst firing and LTCS in TC neurons

A: Representative traces recorded in current-clamp mode from a TC neuron at a holding potential of −76 mV (top panel). LTCS was evoked on injection of a small depolarizing pulse (duration of 160 msec) and elicited a burst of 8 APs. This LTCS and resulting burst were effectively abolished in the presence of 1 mM octanol (middle panel), but were partially recovered on washout of octanol with only two APs (bottom panel), bars indicate calibration. Holding potential was maintained by a constant injection of current *via* the recording electrode. **B**: The histogram in the top panel compares the number of AP spikes in control (5.8 ± 0.7) and in the presence of octanol (0.4 ± 0.2). Asterisk indicates $p < 0.001$ (n = 5 cells, Student t-test). Middle panel indicates that octanol (−78.3 ± 1.4 mV) did not significantly affect baseline (−78.4

± 2.6 mV, n=7, p>0.05) RMP in TC cells. Similarly, bottom panel indicates that octanol (127 ± 12 mΩ) did not significantly affect baseline (126 ± 10 mΩ, n=7, p>0.05) R_{in} in TC cells. Vertical bars represent standard errors. Open bars represent control conditions and cross-hatched bars represent conditions after applications of octanol.

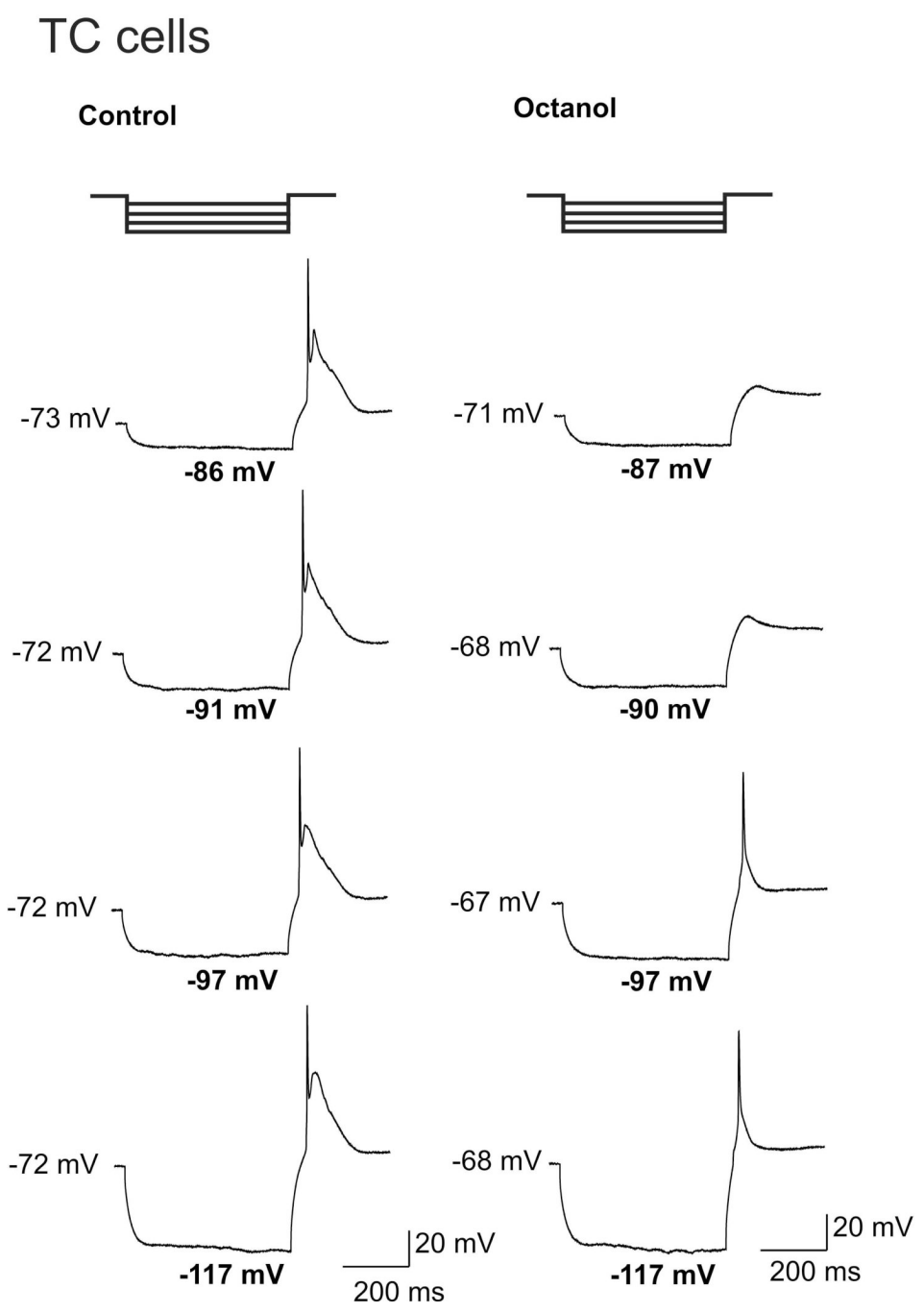

Figure 8. Progressive membrane hyperpolarization partially relieves inhibition of rebound spike firing in TC cells by octanol

Two bold traces on the top illustrate current-clamp protocol used for this experiment in a representative TC cell. Successive traces on the left are obtained in control conditions and on the right after application of 1 mM octanol in the same cell. Traces are chosen to compare the effects of octanol on rebound spike firing at similar hyperpolarized membrane potentials (numbers in bold fonts). Note that there was relatively stable baseline in the control conditions and mild membrane depolarization in the presence of octanol (numbers on the left side of each corresponding trace indicate RMPs). In control conditions this cell fired reliably two spikes. Application of octanol completely abolished spiking at hyperpolarized potentials of −87 mV

and at −90 mV, but with more progressive hyperpolarization at −97 mV and at −117 mV, the cell fired single rebound APs in the presence of octanol. Bars indicate calibration.